ARTICLE

In Situ Growth of Catalytic Active Au—Pt Bimetallic Nanorods in Thermoresponsive Core—Shell Microgels

Yan Lu,[†,*] Jiayin Yuan,[‡] Frank Polzer,[†] Markus Drechsler,[‡] and Johannes Preussner[§]

[†]F—I2 Soft Matter and Functional Materials, Helmholtz-Zentrum Berlin für Materialien und Energie, Hahn-Meitner-Platz 1, 14109 Berlin, Germany, [‡]Makromolekulare Chemie II, University of Bayreuth, 95440 Bayreuth, Germany, and [§]Metallische Werkstoffe, University of Bayreuth, 95440 Bayreuth, Germany

ABSTRACT Here, we demonstrate that bimetallic Au—Pt nanorods (NRs) can be grown *in situ* into thermosensitive core—shell microgel particles by a novel two-step approach. In the first step, Au NRs with an average width of 6.6 ± 0.3 nm and length of 34.5 ± 5.2 nm (aspect ratio 5.2 ± 0.6) were homogeneously embedded into the shell of PNIPA networks. The volume transition of the microgel network leads to a strong red shift of the longitudinal plasmon band of the Au NRs. In the second step, platinum was preferentially deposited onto the tips of Au NRs to form dumbbell-shaped bimetallic nanoparticles. The novel synthesis forms bimetallic Au—Pt NRs immobilized in microgels without impeding their colloidal stability. Quantitative analysis of the catalytic activity for the reduction of 4-nitrophenol indicates that bimetallic Au—Pt NRs show highly enhanced catalytic activity, which is due to the synergistic effect of bimetallic nanoparticles. The catalytic activity of immobilized Au—Pt NRs can be modulated by the volume transition of thermosensitive microgels. This demonstrates that core—shell microgels are capable of serving as "smart nanoreactors" for the catalytic active bimetallic nanoparticles with controlled morphology and high colloidal stability.

KEYWORDS: thermoresponsive · microgel · bimetallic · nanorods · catalysis

Environmentally responsive microgels, which can react in a specific way to external stimuli, have been the subject of great interest in the last two decades due to their versatile applications,[1] such as drug delivery,[2,3] biosensing,[4] chemical separation,[5] and catalysis.[6,7] Recently, polymer—inorganic hybrid microgels comprising metal nanoparticles have become the current research focus because they open new avenues in the synthesis and fabrication of various materials with advanced properties.[8—11] For example, Kumacheva *et al.*[12,13] introduced polymer microgels as carrier systems for different nanoparticles (NPs). They showed that NPs made from semiconductors and metals can be successfully synthesized using these polymer microgels as templates. These systems are expected to have promising applications in catalysis and chemical and biological separation. Kawaguchi *et al.*[14,15] have reported the color change of hybrid microgels loaded with Au or Ag/Au nanoparticles. The color change can be tuned by the interparticle interactions modulated by the swelling or deswelling of the thermosensitive microgel. Very recently, we have demonstrated that thermosensitive core—shell microgels can work as "nanoreactors" for the immobilization of metal nanoparticles that allows us to modulate the catalytic activity of metal nanoparticles by the volume transition that takes place within the carrier system.[16—19] To our best knowledge, so far, only spherical metal nanoparticles have been prepared *via* the *in situ* approach because of the difficulty associated with the morphology control within the microgel matrix.

Considerable attention has been paid to one-dimensional (1-D) inorganic nanomaterials such as nanorods,[20—22] nanotubes,[23] and nanowires[24,25] stemming from their unique size- and shape-dependent optoelectronic and surface properties.[26—28] As one of the most intensively studied 1-D nanomaterials, Au nanorods (Au NRs) show interesting optical properties in the visible and near-infrared (NIR) region because of the strong anisotropy of shape.[29,30] For the preparation of Au nanorods, a synthetic protocol referred to as "seed-mediated growth" has been established by several groups in the past few years.[31,32] Typically, Au NRs carry a positive charge owing to the cationic surfactant cetyltrimethylammonium bromide (CTAB), which is used as the shape-inducing and stabilizing agent of Au NRs. The electrostatic interaction between the positively charged NRs and the negatively charged microgels has been employed for the immobilization of presynthesized Au NRs on the microgels.[33] Furthermore, Hellweg *et al.*[34] demonstrated that, by modification of Au NRs with polyelectrolyte layers, negatively charged thermosensitive poly(*N*-isopropylacrylamide)

*Address correspondence to yan.lu@helmholtz-berlin.de.

Received for review March 22, 2010 and accepted November 5, 2010.

Published online November 17, 2010. 10.1021/nn102622d

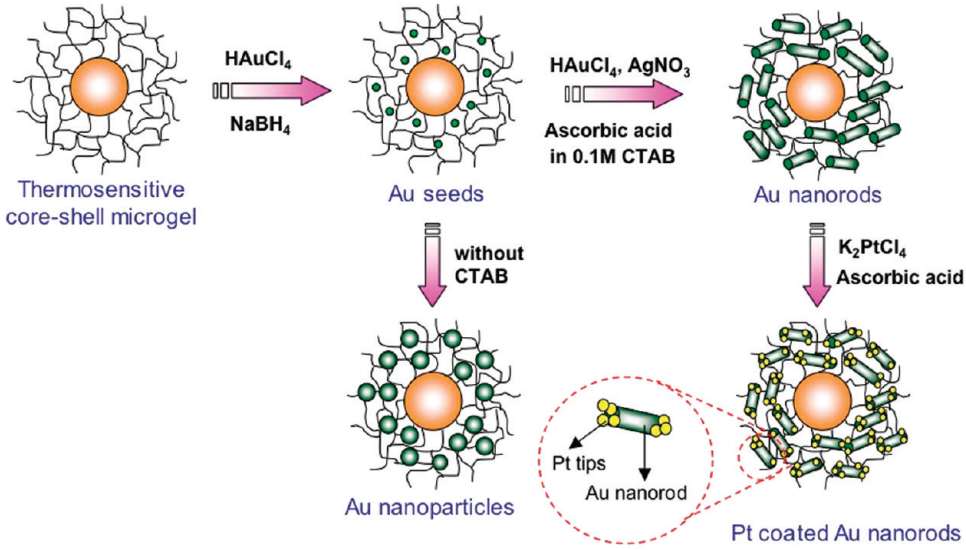

Figure 1. Schematic illustration of the *in situ* generation of bimetallic Au−Pt NRs in the thermosensitive core−shell microgels by means of a seed-mediated growth method.

(PNIPA) microgels can be homogeneously covered with Au NRs. The optical properties of Au NRs were used to monitor the thermoresponsive behavior of the PNIPA microgels. More recently, Kumacheva *et al.*[35] have found that the strong binding forces between Au NRs and polyacryamide microgels is another driving force to load microgels with NRs.

So far, the deposition of Au NRs onto responsive microgels has been achieved mostly by an adsorption process, which requires either modification of Au NRs surface[34,36] or a specific microgel system.[35] In this paper, we introduce for the first time the *in situ* generation of bimetallic Au−Pt NRs within the thermosensitive microgel particles. The present synthetic protocol of the Au−Pt bimetallic particles is an important progression; it demonstrates that the control of the shape as well as hierarchical structure of nanoparticles in the microgel particles is achievable *via* an *in situ* strategy. Compared to the method we developed for the immobilization of spherical Ag nanoparticles,[16] here we extend the concept of microgel particles as "lab on a particle".

Furthermore, comparison to the reported adsorption method, the *in situ* generation of Au NRs within the thermoresponsive microgels is expected to present several advantages: (1) enhanced colloidal stability; (2) higher activity in catalysis or surface enhanced Raman scattering (SERS) when compared to Au nanoparticles stabilized by alkyl chains through thiol bonds or polyelectrolytes, which may alter the properties of the metal profoundly;[37] (3) higher loading capacity because Au NRs are immobilized in the whole microgel network instead of only on the outer surface; (4) readily applicable for preparing other types of anisotropic bimetallic nanoparticles (such as Au−Pd, Au−Ag, Au−Ni, *etc.*) simply by choosing different depositing metals to incorporate new functions to the composite particles.

The microgels studied here consist of a polystyrene core and a network shell made of PNIPA cross-linked by *N*,*N*′-methylenebisacrylamide.[16] The method used for the *in situ* growth of bimetallic Au−Pt NRs in the presence of microgel particles is illustrated in Figure 1. Based on our previous work, thermosensitive microgel particles can be considered as excellent "nanoreactors" for the immobilization of Au nanoparticles.[19] These preformed Au nanoparticles, which act as seeds, direct the growth of Au NRs (seeded-mediated growth) inside the microgel carrier system. The influence of volume transition of microgel particles on the optical properties of the embedded Au NRs investigated by UV−vis spectroscopy will be presented in detail. In the following step, the as-synthesized Au NRs captured within the microgels can be employed as anisotropic seeds for the *in situ* growth of platinum tips, resulting in a strong surface plasmon shift of the Au NRs. Cryo-TEM has been applied to investigate the morphology change of the hybrid particles in solution state throughout the synthetic procedure. In addition, the catalytic activity of microgel-Au NRs before and after deposition of the Pt tips has been tested *via* the reduction of 4-nitrophenol. The influence of temperature on the catalytic activity of microgel composite particles has also been investigated.

RESULTS AND DISCUSSION

As shown in Figure 1, the Au NRs were first synthesized in the presence of thermosensitive microgel particles by the seed-mediated growth. Initially, monodispersed Au nanoparticles with an average diameter of ~5 nm were prepared *via* the reduction of $HAuCl_4$ by $NaBH_4$, and homogeneously immobilized into a microgel template. This can be seen directly in the TEM image (Figure 2a). No secondary Au nanoparticles could be found outside the microgel template. This is due to

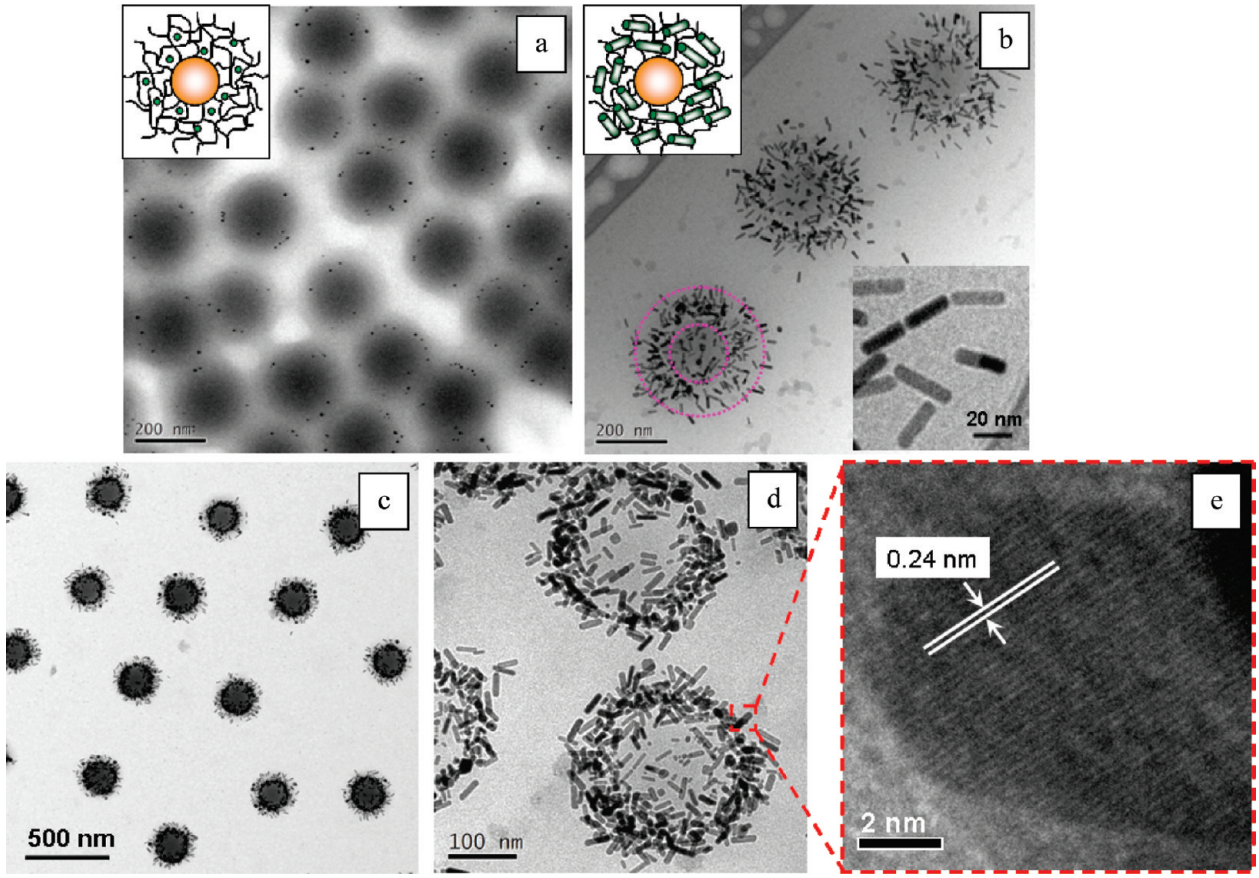

Figure 2. (a) TEM image of Au seeds embedded in microgel particles; (b) Cryo-TEM image of Au NRs growth in the presence of thermosensitive core−shell microgels (Dashed circles indicate the size of the PS core and the microgel particles in swollen state as measured by DLS, respectively ($R_h^{PS\ core}$ = 87.8 nm, $R_h^{microgel}$ = 198.4 nm at 25 °C). The inset shows the morphology of embedded Au NRs.); (c,d) TEM images of Au NRs growth in the presence of microgels; and (e) HRTEM image of Au NRs embedded into microgel particles.

the complexation of the metalate ions with the nitrogen atoms of the PNIPA network[38] and the relatively small amount of the gold precursor ([Au]/[microgel] = 2 wt %). Thus, no purification of the as-synthesized nanoparticles is required. Moreover, the microgel particles are weakly positively charged (zeta potential ~ 19.8 mV at 25 °C) because of the cationic initiator (V50) used in the polymerization. This may facilitate the immobilization of negatively charged $AuCl_4^-$ ions into the positively charged microgel particles.[19,39] Au NRs were generated *in situ* by means of seed-mediated growth using preformed Au nanoparticles deposited in the microgel. Because the Au seeds only exist in the PNIPA networks of the microgel, the growth of Au NRs proceeds exclusively in the microgel. In this step, silver nitrate was added to achieve Au NRs with controlled aspect ratios in a high yield, as reported previously.[31,40] The Au-NR growth process was initiated by adding specific quantities of the microgel-Au seeds into 0.1 M CTAB aqueous solution. The role of CTAB is essential for the formation of nanorods.[29] In a controlled experiment in the absence of CTAB, large spherical Au nanoparticles with an average diameter of ~22 nm were detected in the microgel templates (see Figure S1 in Supporting Information). Additionally, concerning the microgel particles used here are only weakly charged, the electrostatic interactions in the system will not be considered as the main defining forces for the immobilization of Au NRs.[35]

The growth of Au NRs in the presence of microgel-Au seed solutions was monitored by the UV−vis spectroscopy as shown in Figure 3a. Au NRs possess two absorption bands, one at a shorter wavelength (transverse plasmon resonance, around 520 nm) and the other at a longer wavelength (longitudinal plasmon resonance) that undergoes a bathochromic shift with an increasing aspect ratio.[31] We found that the longitudinal plasmon band of Au NRs appeared 2−3 min after the start of the reaction. In the next 10 min, a slow-continuous blue-shift occurred as the Au NRs developed. This phenomenon is in accordance with that observed for the Au-NR growth in the absence of template. It reflects the change of the aspect ratio of the developing Au NRs: the aspect ratio increases quickly in the beginning of the reaction and then slowly decreases over time.[31] In addition, a secondary shoulder at transverse plasmonic band appears with reaction time, which is caused by the faceting of the ends of the Au NRs. This is in accordance with the results observed by Murphy *et al.*[31] Thus, we conclude that the

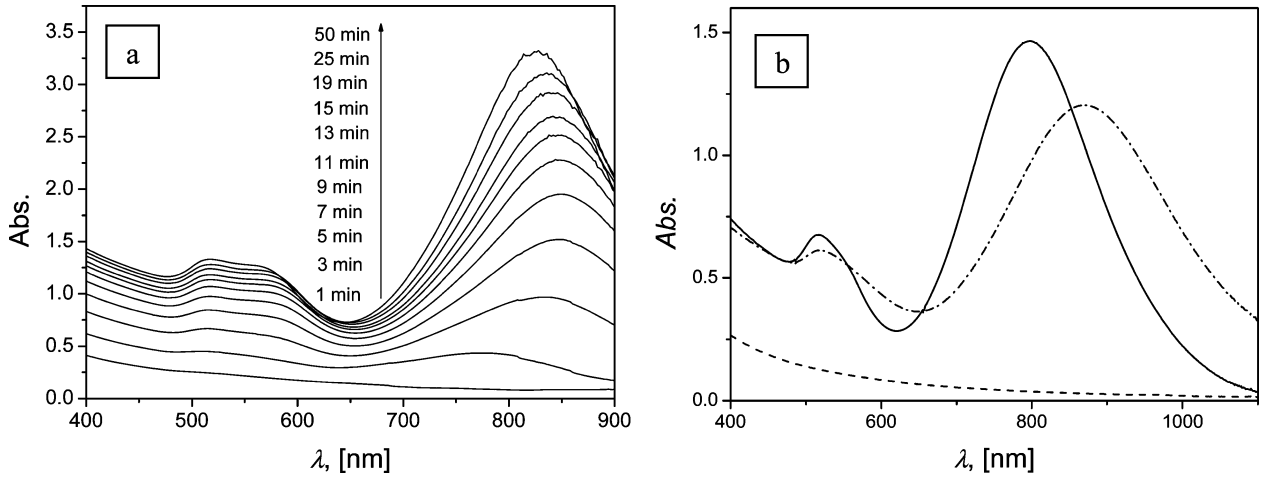

Figure 3. (a) UV−vis spectra of Au NRs solution showing the shift of the Plasmon bands with the growth of the Au seeds as a function of time. (b) UV−vis spectra of Au seeds (dashed line) in the microgel templates after growth of Au NRs nanoparticles (solid line), followed with deposition of Pt tips (chain dotted line).

presence of the microgel template does not disturb the growth of Au NRs. This conclusion was further confirmed by transmission electron microscope (TEM) and cryo-TEM measurements, as shown in Figure 2b−d. Au NRs were found randomly located only in the microgel networks; no free rods are observed in solution. The crystallinity of the Au NRs was checked with high-resolution TEM in Figure 2e, which shows clear lattice fringes with interplanar spacing of 0.24 nm, assigned to the (111) plane of the face-centered-cubic (fcc) crystal structure of gold.

To study the real morphology of microgel/Au NR nanocomposites in solution, that is, in the swollen state, cryo-TEM measurements have been performed. As shown in Figure 2b, the Au NRs are homogeneously immobilized inside the PNIPA network shell. The cores appear as gray spheres. Keep in mind that the cryo-TEM images (Figure 2b) of microgel/Au NR composites show the *in situ* morphology of composite particles, while the TEM images (Figure 2c) display only the dried state. In the dried state the PNIPA shell has shrunk, resulting in a higher local density of Au NRs in the microgel shell, which confirms again that Au NRs have been firmly localized and confined in the PNIPA networks by this *in situ* preparation method. Analysis of the cryo-TEM images indicates that the obtained Au NRs are uniformly sized, with an average width of 6.6 ± 0.3 nm and length of 34.5 ± 5.2 nm (aspect ratio 5.2 ± 0.6).

One important property of Au NRs is their optical response in the visible and near-infrared (NIR) regions.[29] The influence of volume transition of microgel particles on the optical properties of the microgel-Au NRs composite particles has also been investigated in this study. The UV−vis spectra have been recorded for the composite particles in the temperature range between 22 °C (swollen state of the microgel) and 44 °C (collapsed state of microgel) as shown in Figure 4a (LCST of PNIPA = 32 °C). From Figure 4a, it can be observed clearly that there is a red shift of the longitudinal plasmon resonance with increasing temperature. Figure 4b shows that the shift of longitudinal plasmon peak with temperature is directly correlated to the volume transition

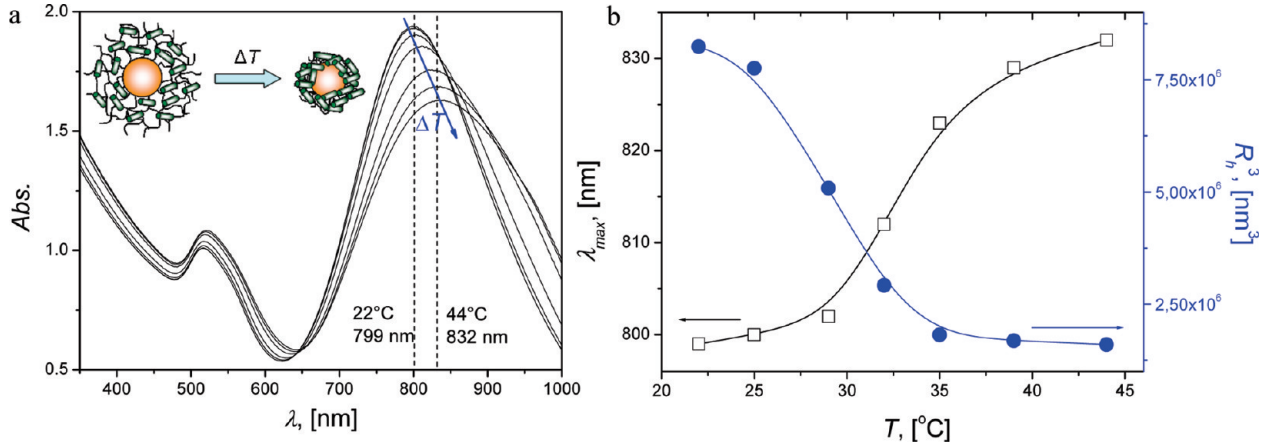

Figure 4. (a) UV−vis spectra of microgel-Au NRs sample at different temperatures (22, 25, 29, 32, 35, 40, and 44 °C). Arrow indicates the increase in temperature. (b) Maximum of the longitudinal plasmon band of microgel-AuNRs composites as a function of temperature (open squares) and the volume transition of the microgel particles (solid circles).

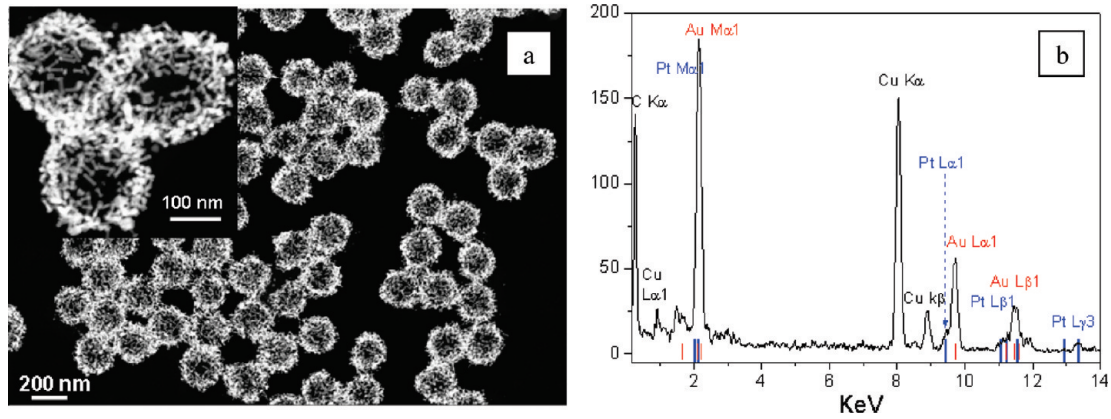

Figure 5. (a) Dark field STEM images of the microgel composite particles and (b) corresponding EDX to prove the elemental composition of Pt on the Au NRs (Cu from the copper grid).

of the network. The longitudinal plasmon peak of Au NRs is centered at ~800 nm at lower temperature and shifted to ~830 nm when the temperature was above 35 °C. It should be noted that this transition is fully reversible upon cooling down to room temperature. The shifting to longer wavelengths and the broadening of the surface plasmon absorption band are attributed to the increase of local refractive index near Au NRs during the collapse of microgel particles.[34] A similar shift induced by the collapse of the microgel has been also found in Ag NP embedded microgels.[7] However, a much higher sensitivity was observed for the Au NRs: The plasmon band shift is around 30 nm when the temperature changes from 20 to 40 °C, while the respective shift for the microgel-Ag nanocomposites is only 6 nm.

An advantage of the *in situ* synthesis is that Au NRs embedded in microgel particles can be used as seeds for further growth or coating with other metals. In the present study, we succeeded in the controlled growth of platinum specifically on the Au NRs embedded in the microgels. This was achieved using ascorbic acid as the reducing agent. As reported in an earlier study by Liz-Marzán *et al.*,[41] platinum will deposit preferentially on the Au NRs tips when Ag^+ ions are present during the deposition procedure. Accordingly in our case, Ag^+ ions were kept in the system after the formation of Au NRs. Figure 3b shows the UV−vis absorption spectra of Au seeds and microgel-Au NR hybrids before and after Pt deposition. As can be seen from Figure 3b, the Au seeds did not display an intensive plasmon resonance due to their small size.[42] After the formation of Au NRs within the microgels, two absorption maxima were observed. The maximum located in the longer wavelength region is characteristic of Au NRs. The growth of Pt on Au NRs was indicated by a significant red-shift in the longitudinal plasmon band ($\Delta\lambda = 75$ nm). The morphology was visualized directly by scanning transmission microscope (STEM) and cryo-TEM measurements as shown in Figure 5a and 6. More TEM images are displayed in Figure S2 in Supporting Information. Platinum is found preferentially deposited on both tips of Au NRs embedded in the microgel particles, thereby leading to the observed dumbbell shape. Preferential platinum deposition on the tips is due to the distribution of Ag^+ on the surface of the gold. The circumambient faces, which are efficiently covered with Ag^+, have a decreased rate of platinum deposition compared to the tip faces, which are only partially covered by silver.[40,41] Energy dispersive X-ray (EDX) measurement has been performed to determine the growth of Pt on Au NRs (Figure 5b). The presence of both Au and Pt signals and the absence of Cl signal confirm that the Pt ions that were added into the microgel-Au NRs solution

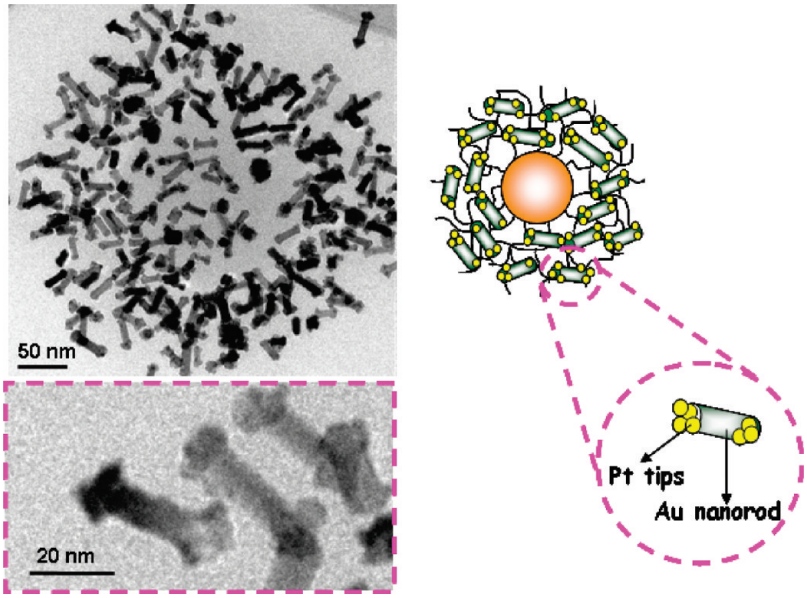

Figure 6. Cryo-TEM image and the enlarged views of Pt tips growth on the Au NRs in water.

have been completely reduced to Pt, forming bimetallic Au−Pt nanorods. Moreover, no secondary Pt nanoparticles were observed either in the microgel template or in the solution, as proven by the STEM and cryo-TEM pictures of the microgel hybrids (Figures 5 and 6). The analysis of the cryo-TEM images indicates that the obtained metallic Au−Pt NRs have an average width (middle) of 7.4 ± 0.8 nm and length of 39.5 ± 6.5 nm (aspect ratio 5.3 ± 0.6). EDX measurement indicates that 17.2 wt % Pt has been deposited onto Au NRs that are immobilized in microgels.

Bimetallic nanoparticles are of great interest in determining chemical reactivity and especially catalytic activity.[43] In our study, the catalytic behavior of microgel-Au NRs before and after Pt deposition has been investigated for the catalytic reduction of 4-nitrophenol by sodium borohydride, which is a benchmark reaction for monitoring the catalytic activity of metal nanoparticles.[44−46] It is worth noting that 4-nitrophenol is one of the most refractory pollutants in industrial wastewaters. Additionally, the reduction of 4-nitrophenol to 4-aminophenol is of industrial importance as an intermediate for the manufacture of analgesic and antipyretic drugs.[7] The kinetics of this reaction can be easily monitored by UV−vis spectroscopy, as shown in Figure S3 in Supporting Information. After the addition of microgel−metal nanocomposites the peak at 400 nm, which is due to the 4-nitrophenate ions, decreases gradually with time and a new peak appears at 290 nm. This peak results from the product 4-aminophenol.[47] Sodium borohydride was used in excess compared to the concentration of 4-nitrophenol so that a first order rate kinetics with regard to the 4-nitrophenol concentration could be used to evaluate the catalytic rate. Controlled experiments using unmodified microgel particles indicated that no reaction occurs in the absence of the metal nanoparticles.

Figure 7 shows the values of the apparent rate constant k_{app} as a function of concentrations of microgel-Au NRs with and without Pt tips. A linear relation between k_{app} and the concentration of Au NRs is observed. Apparently, the bimetallic Au−Pt NRs exhibit higher catalytic activity than that of microgel-Au NRs. Pt nanoparticles are known to act as catalysts for the reduction of 4-nitrophenol. To understand the enhancement of the catalytic activity of microgel-Au NRs after the deposition of Pt tips, two additional samples were investigated: one is microgel-Pt NPs, spherical Pt nanoparticles (d = 3.7 ± 1.2 nm) immobilized in the microgels. (A TEM image of the composite particles is shown in Figure S4 in Supporting Information.) The second is a mixture of microgel-Au NRs and microgel-Pt NPs that contains the same amount of Pt as that in the bimetallic Au−Pt NRs.

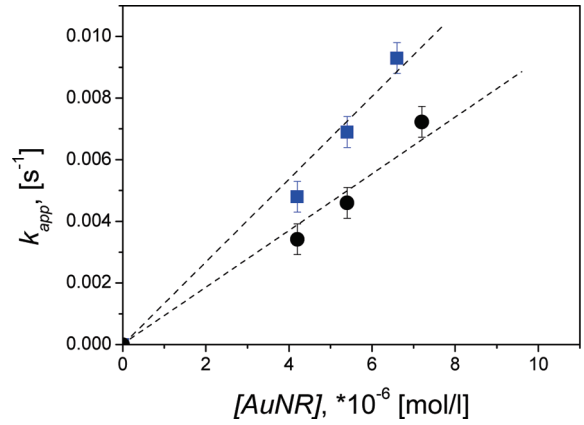

Figure 7. Rate constant k_{app} as a function of concentration of microgel-Au NR composites before (circles) and after (quadrangles) deposition of Pt tips: [4-nitrophenol] = 0.1 mmol/L, [$NaBH_4$] = 10 mmol/L, T = 25 °C.

Moreover, to compare the catalytic activity of the composite particles quantitatively, a parameter k_1, which is the apparent rate constant (k_{app}) normalized to the specific surface area of metal particles (S), has been calculated as the specific turnover frequencies for different systems:[48]

$$-\frac{dc_t}{dt} = k_{app}c_t = k_1 S c_t \qquad (1)$$

where c_t is the concentration of 4-nitrophenol at time t, and k_1 is the rate constant normalized to S, the surface area of metal nanoparticles normalized to the unit volume of the system.

Figure 8 shows the values of the apparent rate constant k_{app} as a function of theoretical specific metal particle surface area of different samples. First of all, it is obvious from Figure 8 that Pt NPs immobilized in microgels can work as catalyst for the reduction of 4-nitrophenol. However, its catalytic activity (k_1 = 0.086 s^{-1} m^{-2} L) is lower than that of Au NRs (k_1 = 0.14 s^{-1} m^{-2} L) and much lower than that of Au-Pt NRs (k_1 =

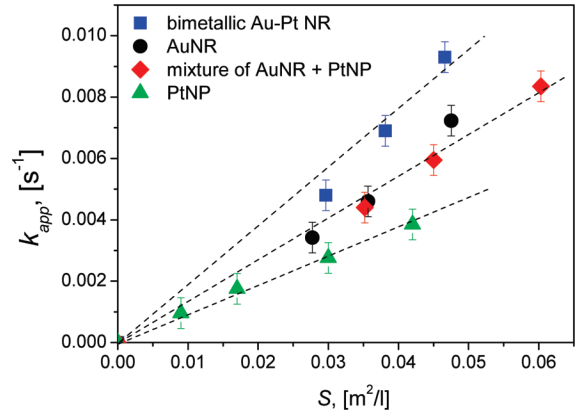

Figure 8. Rate constant k_{app} as a function of surface area S of metal nanoparticles normalized to the unit volume of the system: [4-nitrophenol] = 0.1 mmol/L, [$NaBH_4$] = 10 mmol/L, T = 25 °C; circles, microgel-Au NR composites; quadrangles, microgel−Au-Pt NR composites; triangles, microgel−Pt NP composites; diamonds, mixture of microgel−Au NR with microgel−Pt NP.

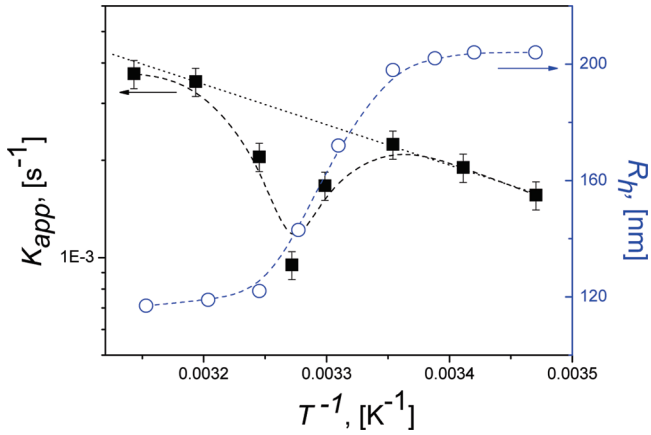

Figure 9. Arrhenius plot of the reaction rate k_{app}. Quadrangles give the reaction rate k_{app} measured in presence of microgel−Au-Pt NRs at different temperatures. Open circles present the change of the hydrodynamic radius (R_h) of microgel composite particles with temperature.

0.21 s^{-1} m^{-2} L). Second, it is interesting to find that the mixture of microgel-Au NRs and microgel-Pt NPs does not show an increase in catalytic activity compared to the microgel−Au-Pt NRs composite particles. Because the amount of Pt in the mixture is the same as that in the bimetallic Au-Pt NRs, this indicates that the enhancement of the catalytic activity is due to the synergistic effect of bimetallic Au-Pt NRs. Recently, Sönnichsen *et al.*[49] have reported the improvement of the catalytic activity of rod-shaped gold nanorattles after replacing the Au shell with Pd. In the present work, the enhancement of the catalytic activity of Au NRs after the deposition of Pt tips has been proved.

An obvious advantage of the "*in situ*" preparation of bimetallic Au-Pt NRs using thermosensitive microgels as a carrier system is that microgel particles can work as "active" carriers that can modulate the catalytic activity of embedded metal nanoparticles through the volume transition of the thermosensitive microgel shell.[16,17] In the last part of the present study, we have demonstrated this concept by measuring the catalytic rate of microgel−Au-Pt NRs at different temperatures. As shown in Figure 9, the rate constants k_{app} obtained at different temperatures for bimetallic Au-Pt NRs prepared by thermosensitive microgel particles do not follow the typical Arrhenius-type dependence on temperature. When the reaction temperature is higher than 25 °C, the PNIPA-network shrinks markedly with the increase of temperature as indicated in Figure 9 by plotting the hydrodynamic radius R_h as the function of 1/*T*. The change of temperature leads to the shrinking of the PNIPA network, which is followed by a concomitant slowing down of the diffusion of reactants within the network. This in turn decreases the rate constant k_{app} catalyzed by the bimetallic Au-Pt NRs, which is similar to the result obtained for metal nanoparticles immobilized in microgel particles.[18] Further increases in temperature do not result in additional shrinking of the PNIPA network. At this point, the large increase of k_{app} with *T* overcomes the hindered diffusion and the reaction rate rises again. Thus, the rate constant k_{app} must reach its minimum at the transition temperature as shown in Figure 9. This demonstrates the first time that the catalytic activity of complex nanostructures immobilized within the thermosensitive microgels can be modulated by the volume transition of the carrier system.

CONCLUSIONS

We demonstrate that bimetallic Au-Pt NRs can be grown *in situ* and embedded into thermosensitive core−shell microgel particles by a novel two-step approach. First, Au NRs with an average width of 6.6 ± 0.3 nm and length of 34.5 ± 5.2 nm (aspect ratio 5.2 ± 0.6) have been homogeneously embedded into the shell of PNIPA networks. The volume transition of the microgel network leads to a strong red shift of the longitudinal plasmon band of the Au NRs. Then platinum can be preferentially deposited onto the tips of Au NRs embedded in microgel particles to form dumbbell-shaped bimetallic nanoparticles. This novel synthesis forms bimetallic Au-Pt NRs immobilized in microgel particles without impeding their colloidal stability or thermosensitivity. Quantitative analysis indicates that the catalytic activity of Au NRs is significantly enhanced after the deposition of Pt tips for the catalytic reduction of 4-nitrophenol. In addition, the catalytic activity of bimetallic Au-Pt NRs nanocomposites can be modulated by the volume transition of microgel particles. The present study has demonstrated the general ability of core−shell microgels to serve as "active" reactors leading to complex multifunctional nanostructures *via* "*in situ*" approach, which could create new opportunities for nanotechnologies.

METHODS

Chemicals and Materials. *N*-Isopropylacrylamide (NIPA; Aldrich), *N*,*N*′-methylenebisacrylamide (BIS; Fluka), sodium dodecyl sulfate (SDS; Fluka), potassium peroxodisulfate (KPS; Fluka), cetyltrimethylammonium bromide (CTAB; Aldrich), 2,2′-azobis(2-methylpropionamidine dihydrochloride) (V50; Aldrich), ascorbic acid (AA; Fluka), silver nitrate ($AgNO_3$; Aldrich), sodium borohydride ($NaBH_4$; Aldrich), tetrachloroauric acid trihydrate ($HAuCl_4 \cdot 3H_2O$; Aldrich), and potassium tetrachloroplatinate(II) (K_2PtCl_4; Aldrich) were used as received. Styrene (BASF) was destabilized by an Al_2O_3 column and stored in the refrigerator.

Synthesis of Thermosensitive Core−Shell Microgel Particles. In the first step, PS core latex was prepared by conventional seeded emulsion polymerization, which was reported previously.[19] The PS-NIPA core−shell system was prepared by seeded emulsion polymerization. PS core latex (7.67 g) was diluted with 240 g of water together with 8.367 g of NIPA and 0.286 g of BIS. After that, the mixture was heated to 80 °C. The reaction was started with the addition of 0.30 g of V50 (dissolved in 10 g of water) and continued for 4.5 h. The latex was purified by serum replacement against deionized water (membrane: cellulose nitrate with 100 nm pore size supplied by Schleicher and Schuell).

Synthesis of Au Nanorods in the Presence of Microgel Particles. Gold seeds and nanorods were prepared using a wet-chemical

method modified from the method described by Murphy *et al.*[31] Initially, Au seeds were prepared in the presence of microgel particles. In a typical experiment, 0.2733 g CTAB was first dissolved in 5.32 mL water. Then 2.179 g microgel solution (solid content 2.295 wt %), 0.025 mL of 0.01 M $HAuCl_4$ was added to a glass test tube with gentle stirring. After that, 0.6 mL of an aqueous 0.01 M ice-cold $NaBH_4$ solution was added at once, followed by rapid magnetic stirring for 2 min. The seed solution was kept at 25 °C for 2 h before using.

For the preparation of Au nanorods, 9.5 mL of 0.1 M CTAB, 0.4 mL of 0.01 M $HAuCl_4$, and 0.06 mL of 0.01 M $AgNO_3$ solutions were added in that order, to a glass test tube, followed by gentle mixing. Then 0.064 mL of 0.1 M AA solution was added to it. The solution became colorless upon addition and mixing of AA. Finally, 0.1 mL of as-prepared seed solution was added, and the reaction mixture was gently mixed for 10 s and left undisturbed at 25 °C for at least 3 h. After that, the solution was washed by centrifugation (8500 rpm, 10 min) and redispersed in a desired amount of Milli-Q water.

Growth of Platinum on Au Nanorods Embedded in Microgel Particles. The deposition of platinum on Au nanorods was modified from the method developed by Liz-Marzán *et al.*[41] In a typical run, to 5 mL of as-prepared microgel−Au NRs solution, 5 mL of 0.1 M CTAB and 0.05 mL of 0.01 M K_2PtCl_4 were added at 28 °C, and the mixture was left for 1 h to allow for complexation of the platinum salt with CTAB. Followed by addition of 0.1 mL of 0.1 M AA, the solution was maintained at 28 °C for 36 h to ensure complete reduction. In the end, Pt coated microgel−Au NRs were washed by centrifugation (8000 rpm, 10 min) and redispersed in desired amount of Milli-Q water.

Catalytic Reduction of 4-Nitrophenol. A total of 0.5 mL of sodium borohydride solution (60 mmol/L) was added to 2.5 mL of 4-nitrophenol solution (0.12 mmol/L) contained in a glass vessel. After that, a given amount of the composite particles was added. Immediately after the addition of the composite particles, UV spectra of the sample were taken every 30 s in the range of 250−550 nm. The rate constant of the reaction was determined by measuring the change in intensity of the peak at 400 nm with time. For the calculation of the total surface of Au nanorods, which is a decisive parameter and used in kinetic analysis, the size of the Au nanorods is determined by the analysis of TEM micrographs, assuming cylindrical particles (width of 6.6 nm and length of 34.5 nm). The amount of Au in the composites is 13.7 wt % determined by thermogravimetric measurements (TGA). In the case of Pt nanoparticles, the size is determined by the analysis of TEM micrographs, assuming spherical particles ($d = 3.7$ nm). In the case of bimetallic Au-Pt NRs, cylindrical Au NRs deposited with spherical Pt nanoparticles ($d = 5.6$ nm) are assumed (see in scheme in Figure 1). The content of Pt in the bimetallic Au-Pt particles is 17.2 wt % by EDX measurements. The bulk density of Au ($\rho = 19.32 \times 10^3$ kg/m^3) and Pt ($\rho = 21.45 \times 10^3$ kg/m^3) have been used for the density of Au and Pt nanoparticles, respectively.

Instrumentation. Cryogenic transmission electron microscopy was carried out as outlined in ref 50. STEM images and EDX measurements were done in a Zeiss Libra 200FE with in-lens energy filter. Dynamic light scattering measurements were conducted using an ALV 4000 light scattering goniometer (Peters, Langen, Germany) at the angle of 90°. The UV−vis spectra were measured by Lambda 650 spectrometer supplied by Perkin-Elmer or an Agilent 8453 spectrophotometer with a temperature-controlled sample holder with an accuracy of ±0.1 °C. The amount of metal immobilized in the microgels was determined by TGA using a Mettler Toledo STARe system. The samples were first dried under vacuum at 50 °C. Then about 8 mg of the solid composite particles was heated to 800 °C under a 60 mL/min nitrogen flow with a heating rate of 10 °C/min and holding temperature at 800 °C for about 30 min.

Acknowledgment. We thank Prof. M. Ballauff (F−I2, Helmholtz Zentrum Berlin für Materialien und Energie) and Prof. T. Hellweg (PCI, University of Bayreuth) for helpful discussions, Dr. A. Becker (F−I2, Helmholtz Zentrum Berlin für Materialien und Energie) for the critical reading of the manuscript, Prof. Dr.-Ing. U. Glatzel (Metallische Werkstoffe, University of Bayreuth) for providing the TEM instrument, Zeiss Libra 200FE. The authors thank the Deutsche Forschungsgemeinschaft, Schwerpunktprogramm "Hydrogele" (SPP1259) for financial support.

Supporting Information Available: TEM image of Au nanoparticles growth in the thermosensitive core−shell microgels without CTAB, TEM, and cryo-TEM images of Pt tips growth on the Au-NRs embedded in thermosensitive core−shell microgels, UV−vis spectra of solutions of 4-nitrophenol measured at different times, *t*, indicated in the graph in the presence of microgel−Au-Pt NRs solution, and TEM image of Pt nanoparticles embedded in the thermosensitive core−shell microgels. This material is available free of charge *via* the Internet at http://pubs.acs.org.

REFERENCES AND NOTES

1. Stuart, M. A. C.; Huck, W. T. S.; Genzer, J.; Müller, M.; Ober, C.; Stamm, M.; Sukhorukov, G. B.; Szleifer, I.; Tsukruk, V. V.; Urban, M. Emerging Applications of Stimuli-Responsive Polymer Materials. *Nat. Mater.* **2010**, *9*, 101–113.
2. Das, M.; Mardyani, S.; Chan, W. C. W.; Kumacheva, E. Biofunctionalized pH-Responsive Microgels for Cancer Cell Targeting: Rational Design. *Adv. Mater.* **2006**, *18*, 80–83.
3. Soppimath, K. S.; Tan, D. C. W.; Yang, Y. pH-Triggered Thermally Responsive Polymer Core-Shell Nanoparticles for Drug Delivery. *Adv. Mater.* **2005**, *17*, 318–323.
4. Hu, Z.; Chen, Y.; Wang, C.; Zheng, Y.; Li, Y. Polymer Gels with Engineered Environmentally Responsive Surface Patterns. *Nature* **1998**, *393*, 149–152.
5. Kawaguchi, H.; Fujimoto, K. Smart Latexes for Bioseparation. *Bioseparation* **1999**, *7*, 253–258.
6. Biffis, A.; Orlandi, N.; Corain, B. Microgel-Stabilized Metal Nanoclusters: Size Control by Microgel Nanomorphology. *Adv. Mater.* **2003**, *15*, 1551–1555.
7. Lu, Y.; Mei, Y.; Drechsler, M.; Ballauff, M. Thermosensitive Core-Shell Particles as Carrier Systems for Metallic Nanoparticles. *J. Phys. Chem. B* **2006**, *110*, 3930–3937.
8. Ivarez-Puebla, R. A.; Contreras-Cáceres, R.; Pastoriza-Santos, I.; Pérez-Juste, J.; Liz-Marzán, L. M. Au@pNIPAM Colloids as Molecular Traps for Surface-Enhanced, Spectroscopic, Ultra-Sensitive Analysis. *Angew. Chem., Int. Ed.* **2009**, *48*, 138–143.
9. Schrinner, M.; Ballauff, M.; Talmon, Y.; Kauffmann, Y.; Thun, J.; Möller, M.; Breu, J. Single Nanocrystals of Platinum Prepared by Partial Dissolution of Au-Pt Nanoalloys. *Science* **2009**, *323*, 617–620.
10. Hain, J.; Schrinner, M.; Lu, Y.; Pich, A. Design of Multicomponent Microgels by Selective Deposition of Nanomaterials. *Small* **2008**, *11*, 2016–2024.
11. Singh, N.; Lyon, L. A. Au Nanoparticle Templated Synthesis of pNIPAm Nanogels. *Chem. Mater.* **2007**, *19*, 719–726.
12. Zhang, J.; Xu, S.; Kumacheva, E. Photogeneration of Fluorescent Silver Nanoclusters in Polymer Microgels. *Adv. Mater.* **2005**, *17*, 2336–2340.
13. Zhang, J.; Xu, S.; Kumacheva, E. Polymer Microgels: Reactors for Semiconductor, Metal and Magnetic Nanoparticles. *J. Am. Chem. Soc.* **2004**, *126*, 7908–7914.
14. Suzuki, D.; Kawaguchi, H. Gold Nanoparticle Localization at the Core Surface by Using Thermosensitive Core-Shell Particles as a Template. *Langmuir* **2005**, *21*, 12016–12024.
15. Suzuki, D.; Kawaguchi, H. Hybrid Microgels with Reversibly Changeable Multiple Brilliant Color. *Langmuir* **2006**, *22*, 3818–3822.
16. Lu, Y.; Mei, Y.; Drechsler, M.; Ballauff, M. Thermosensitive Core-Shell Particles as Carriers for Ag Nanoparticles: Modulating the Catalytic Activity by a Phase Transition in Networks. *Angew. Chem.* **2006**, *118*, 827−830. *Angew. Chem., Int. Ed.* **2006**, *45*, 813−816.
17. Ballauff, M.; Lu, Y. Smart" Nanoparticles: Preparation, Characterization and Applications. *Polymer* **2007**, *48*, 1815–1823.
18. Mei, Y.; Lu, Y.; Polzer, F.; Ballauff, M.; Drechsler, M. Catalytic Activity of Palladium Nanoparticles Encapsulated in Spherical Polyelectrolyte Brushes and Core-Shell-Microgels. *Chem. Mater.* **2007**, *19*, 1062–1069.

19. Lu, Y.; Proch, S.; Schrinner, M.; Drechsler, M.; Kempe, R.; Ballauff, M. Thermosensitive Core-Shell Microgel as a "Nanoreactor" for Catalytic Active Metal Nanoparticles. *J. Mater. Chem.* **2009**, *19*, 3955–3961.
20. Grzelczak, M.; Pérez-Juste, J.; Mulvaney, P.; Liz-Marzán, L. M. Shape Control in Gold Nanoparticle Synthesis. *Chem. Soc. Rev.* **2008**, *37*, 1783–1791.
21. Yuan, J.; Schmalz, H.; Xu, Y.; Miyajima, N.; Drechsler, M.; Möller, M. W.; Schacher, F.; Müller, A. H. E. Room-Temperature Growth of Uniform Tellurium Nanorods and the Assembly of Tellurium or Fe_3O_4 Nanoparticles on the Nanorods. *Adv. Mater.* **2008**, *20*, 947–952.
22. Xiong, Y.; Cai, H.; Wiley, B. J.; Wang, J.; Kim, M. J.; Xia, Y. Synthesis and Mechanistic Study of Palladium Nanobars and Nanorods. *J. Am. Chem. Soc.* **2007**, *129*, 3665–3675.
23. Tahir, M. N.; Zink, N.; Eberhardt, M.; Therese, H. A.; Kolb, U.; Theato, P.; Tremel, W. Covalent Functionalization through Complexation: WS2 Nanotubes Functionalized with TiO_2 Anatase Nanoparticles. *Small* **2007**, *3*, 829–834.
24. Yuan, J.; Xu, Y.; Walther, A.; Bolisetty, S.; Schumacher, M.; Schmalz, H.; Ballauff, M.; Müller, A. H. E. Water-Soluble Organo-Silica Hybrid Nanowires. *Nat. Mater.* **2008**, *7*, 718–722.
25. Doh, Y. J.; Maher, K. N.; Ouyang, L.; Yu, C. L.; Park, H.; Park, J. Electrically Driven Light Emission from Individual CdSe Nanowires. *Nano Lett.* **2008**, *8*, 4552–4556.
26. Hu, J.; Odom, T. W.; Lieber, C. M. Chemistry and Physics in One Dimension: Synthesis and Properties of Nanowires and Nanotubes. *Acc. Chem. Res.* **1999**, *32*, 435–445.
27. El-Sayed, M. Some Interesting Properties of Metals Confined in Time and Nanometer Space of Different Shapes. *Acc. Chem. Res.* **2001**, *34*, 257–264.
28. Talapin, D. V.; Nelson, J. H.; Shevchenko, E. V.; Aloni, S.; Sadtler, B.; Alivisatos, A. P. Seeded Growth of Highly Luminescent CdSe/CdS Nanoheterostructures with Rod and Tetrapod Morphologies. *Nano Lett.* **2007**, *7*, 2951–2959.
29. Pérez-Juste, J.; Pastoriza-Santos, I.; Liz-Marzán, L. M.; Mulvaney, P. Gold Nanorods: Synthesis, Characterization and Applications. *Coord. Chem. Rev.* **2005**, *249*, 1870–1901.
30. Bardhan, R.; Grady, N. K.; Cole, J. R.; Joshi, A.; Halas, N. Fluorescence Enhancement by Au Nanostructures: Nanoshells and Nanorods. *ACS Nano* **2009**, *3*, 744–752.
31. Sau, T. K.; Murphy, C. J. Seeded High Yield Synthesis of Short Au Nanorods in Aqueous Solution. *Langmuir* **2004**, *20*, 6414–6420.
32. Nikoobakht, B.; El-Sayed, M. A. Preparation and Growth Mechanism of Gold Nanorods (NRs) Using Seed-Mediated Growth Method. *Chem. Mater.* **2003**, *15*, 1957–1962.
33. Gorelikov, I.; Field, L. M.; Kumacheva, E. Hybrid Microgels Photoresponsive in the Near-Infrared Spectral Range. *J. Am. Chem. Soc.* **2004**, *126*, 15938–15939.
34. Karg, M.; Pastoriza-Santos, I.; Pérez-Juste, J.; Hellweg, T.; Liz-Marzán, L. M. Nanorod-Coated PNIPAM Microgels: Thermoresponsive Optical Properties. *Small* **2007**, *7*, 1222–1229.
35. Das, M.; Mordoukhovski, L.; Kumacheva, E. Sequestering Gold Nanorods by Polymer Microgels. *Adv. Mater.* **2008**, *20*, 2371–2375.
36. Karg, M.; Lu, Y.; Carbó-Argibay, E.; Pastoriza-Santos, I.; Pérez-Juste, J.; Liz-Marzán, L. M.; Hellweg, T. Multi-Responsive Hybrid Particles Based on Gold Nanorods and Poly(NIPAM-*co*-allyl-acetic acid) Microgels: Temperature- and pH-Tunable Plasmon Resonance. *Langmuir* **2009**, *25*, 3163–3167.
37. Astruc, D.; Lu, F.; Aranzaes, R. Nanoparticles as Recyclable Catalysts: the Fast-growing Frontier between Homogeneous and Heterogeneous Catalysts. *Angew. Chem., Int. Ed.* **2005**, *44*, 7852–7872.
38. Frattini, A.; Pellegri, N.; Nicastro, D.; de Sanctis, O. Effect of Amine Groups in the Synthesis of Ag Nanoparticles Using Aminosilanes. *Mater. Chem. Phys.* **2005**, *94*, 148–152.
39. Lu, Y.; Mei, Y.; Walker, R.; Ballauf, M.; Drechsler, M. "Nano-Tree"-Type Spherical Polymer Brush Particles as Templates for Metallic Nanoparticles. *Polymer* **2006**, *47*, 4985–4995.
40. Liu, M.; Guyot-Sionnest, P. Mechanism of Silver(I)-Assisted Growth of Gold Nanorods and Bipyramids. *J. Phys. Chem. B* **2005**, *109*, 22192–22200.
41. Grzelczak, M.; Pérez-Juste, J.; Rodríguez-González, B.; Liz-Marzán, L. Influence of Silver Ions on the Growth Mode of Platinum on Gold Nanorods. *J. Mater. Chem.* **2006**, *16*, 3946–3951.
42. Suzuki, D.; McGrath, J. G.; Kawaguchi, H.; Lyon, L. A. Colloidal Crystals of Thermosensitive, Core/Shell Hybrid Microgels. *J. Phys. Chem. C* **2007**, *111*, 5667–5672.
43. Ferrando, R.; Jellinek, J.; Johnston, R. L. Nanoalloys: From Theory to. Applications of Alloy Clusters and Nanoparticles. *Chem. Rev.* **2008**, *108*, 845–910.
44. Pradhan, N.; Pal, A.; Pal, T. Silver Nanoparticle Catalyzed Reduction of Aromatic Nitro Compounds. *Colloids Surf., A* **2002**, *196*, 247–257.
45. Lu, Y.; Mei, Y.; Schrinner, M.; Ballauff, M.; Moller, M. W.; Breu, J. *In Situ* Formation of Ag Nanoparticles in Spherical Polyacrylic Acid Brushes by UV Irradiation. *J. Phys. Chem. C* **2007**, *111*, 7676–7681.
46. Zeng, J.; Zhang, Q.; Chen, J.; Xia, Y. A Comparison Study of the Catalytic Properties of Au-Based Nanocages, Nanoboxes, and Nanoparticles. *Nano Lett.* **2010**, *10*, 30–35.
47. Gosh, S. K.; Mandal, M.; Kundu, S.; Nath, S.; Pal, T. Bimetallic Pt-Ni Nanoparticles Can Catalyze Reduction of Aromatic Nitro Compounds by Sodium Borohydride in Aqueous Solution. *Appl. Catal., A* **2004**, *268*, 61–66.
48. Wunder, S.; Polzer, F.; Lu, Y.; Yu, M.; Ballauff, M. Kinetic Analysis of Catalytic Reduction of 4-Nitrophenol by Metallic Nanoparticles immobilized in Spherical Polyelectrolyte Brushes. *J. Phys. Chem. C* **2010**, *114*, 8814–8820.
49. Khalavka, Y.; Becker, J.; Sönnichsen, C. Synthesis of Rod-Shaped Gold Nanorattles with Improved Plasmon Sensitivity and Catalytic Activity. *J. Am. Chem. Soc.* **2009**, *131*, 1871–1875.
50. Wittemann, A.; Drechsler, M.; Talmon, Y.; Ballauff, M. High Elongation of Polyelectrolyte Chains in the Osmotic Limit of Spherical Polyelectrolyte Brushes: A Study by Cryogenic Transmission Electron Microscopy. *J. Am. Chem. Soc.* **2005**, *127*, 9688–9689.